Designing of Quasi One-Dimensional Acoustic Filters Using Genetic Algorithm

Sebastian GARUS
Institute of Mechanics and Fundamentals of Machinery Design, Czestochowa University of Technology, ul. Dąbrowskiego 73, 42-201 Częstochowa, Poland, gari.sg@gmail.com

Wojciech SOCHACKI
Institute of Mechanics and Fundamentals of Machinery Design, Czestochowa University of Technology, ul. Dąbrowskiego 73, 42-201 Częstochowa, Poland, w.sochacki@imipkm.pcz.pl

Abstract

In phononic quasi one-dimensional structures, there is a phenomenon of a phononic bandgap (PhBG), which means that waves of a given frequency do not propagate in the structure. The location and size of PhBG depend on the thickness of the layers, the type of materials used and their distribution in space. The theoretical study examined the transmission properties of quasi one-dimensional structures designed using a genetic algorithm (GA). The objective function minimized the transmission integral and integral of the absolute value of the transmission functions derivative (to eliminate high transmission peaks with a small half width) in a given frequency range. The paper shows the minimization of transmission in various frequency bands for a 40-layer structure. The distribution of multilayer structure transmission was obtained through the Transfer Matrix Method (TMM) algorithm. Structures surrounded by water were analyzed and built of layers of glass and epoxy resin.

Keywords: acoustic filters, genetic algorithm, transfer matrix

1. Introduction

The beginnings of research on multilayer structures date back to the eighties of the last century [1, 2]. So far, the properties of multilayer structures for mechanical and electromagnetic waves have been analyzed [3-7]. The incident mechanical wave on the multilayer system propagates in it, but on each boundary of the layers there is a partial reflection. Due to multiple reflections and interference, the wave coming out of the system has different characteristics than the incident wave. For the assumed structure, waves of certain frequencies do not propagate through superlattice. This phenomenon is called phononic bandgap (PnBG). The location and size of the forbidden gap depends, among others, on the materials used, the thickness of individual layers, their distribution in space and the surrounding material [8-12]. Due to the structure, phononic (PnC) crystals with batch, quasiperiodic and aperiodic distribution are studied [6, 11, 12]. Phononic crystals can be one-, two- and three-dimensional. Various computational techniques are used to study the transmission properties of photonic crystals, such as Transfer Matrix Method (TMM) [13, 14], Finite Difference Time Domain algorithm (FDTD) [15-17] with Discrete Fourier Transform (DFT) [14], Green's functions [4, 5] and other. The special properties of multi-layer structures allow their use to noise control devices, acoustic and elastic filters, sensors, selective acoustic filters [18-24].

In the work, TMM algorithm was used to determine the transmission of multilayer structures. The propagation of the mechanical wave in layer i is determined by the equation

$$\frac{1}{v_i^2}\frac{\partial^2 p}{\partial t^2} - \nabla^2 p = 0 \tag{1}$$

where p is the pressure of an acoustic wave, t is a time and v_i is a phase velocity. In the case of a quasi one-dimensional structure, the solution to the above equation takes the form

$$p_i = \left(A_i e^{ik_i x} + B_i e^{-ik_i x}\right) e^{-i\omega t} = P_i(x) e^{-i\omega t} \tag{2}$$

Coefficients A_i and B_i describe respectively the wave propagating in accordance with the direction of propagation of the incident wave and the wave propagating in the opposite direction in a given layer i. The wave vector k_i of a given layer depends directly on the frequency f through

$$k_i = \frac{2\pi f}{v_i} \tag{3}$$

The transmission T for a given frequency can be determined directly from the characteristic matrix M of the structure as

$$T = \left|\frac{1}{\mathrm{M}_{1,1}}\right|^2 \tag{4}$$

Mechanical wave propagation is described by the matrix equation (5) in which P_{in}^{+} is incident wave, P_{in}^{-} reflected and P_{out}^{+} transmitted.

$$\begin{bmatrix} P_{in}^{+} \\ P_{in}^{-} \end{bmatrix} = \mathrm{M} \begin{bmatrix} P_{out}^{+} \\ 0 \end{bmatrix} \tag{5}$$

The characteristic matrix is defined as

$$\mathrm{M} = \Phi_{in,1}\left[\prod_{i=2}^{n} \Phi_{i-1,i}\Gamma_i\right]\Phi_{n,out} \tag{6}$$

and consists of a matrix Γ_i describing propagation in a single layer i for a given thickness d_i as

$$\Gamma_i = \begin{bmatrix} e^{ik_i d_i} & 0 \\ 0 & e^{-ik_i d_i} \end{bmatrix} \tag{7}$$

and $\Phi_{i,i+1}$ transmission matrix on the border of i and $i+1$ layers, where ρ is the mass density of the appropriate layer, defined by

$$\Phi_{i,i+1} = \frac{1}{2}\begin{bmatrix} \dfrac{v_{i+1}\rho_{i+1} + v_i\rho_i}{v_{i+1}\rho_{i+1}} & \dfrac{v_{i+1}\rho_{i+1} - v_i\rho_i}{v_{i+1}\rho_{i+1}} \\ \dfrac{v_{i+1}\rho_{i+1} - v_i\rho_i}{v_{i+1}\rho_{i+1}} & \dfrac{v_{i+1}\rho_{i+1} + v_i\rho_i}{v_{i+1}\rho_{i+1}} \end{bmatrix} \tag{8}$$

The transmission properties of the structure largely depend on the distribution of individual material layers. The genetic algorithm (GA) is used to optimize the distribution of the phononic crystals structure [25, 26]. In this work, GA will be used to optimize the distribution of layers, and the scheme of its operation is shown in Fig. 1.

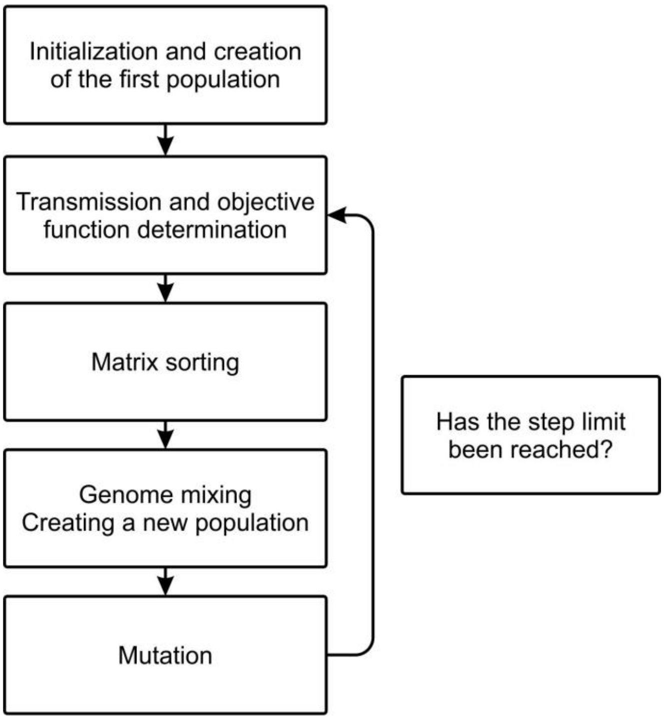

Figure 1. A flowchart of genetic algorithm

Initially, the algorithm's work environment is initialized and a preliminary population is created. Then the transmission of each structure is determined using the TMM algorithm and the value of the objective function is determined based on the formula

$$F_C = \left\| \int_{f_{\min}}^{f_{\max}} T(f)df \right\| \cdot \left\| \int_{f_{\min}}^{f_{\max}} \left| \frac{\partial T(f)}{\partial f} \right| df \right\| \tag{9}$$

The first normalized term is responsible for minimizing the value of the transmission function in a given frequency range, and the second minimizes the possibility of high transmission peaks with a small half width. Equation (9) was used to compare structures in a given population, while function (10) should be used to compare structures between populations.

$$F'_C = \int_{f_{\min}}^{f_{\max}} T(f)df \cdot \int_{f_{\min}}^{f_{\max}} \left| \frac{\partial T(f)}{\partial f} \right| df \tag{10}$$

Then a new population is built based on the sorted structures array by objective function and mixed (the two best structures remain unchanged), after which it undergoes a mutation process with a 1% chance of changing genes. Then the value of the objective function of the new population is determined again and the cycle is repeated. After a certain number of steps, the algorithm stops.

$$F_T = \frac{100\%}{T_{\max} f_{\max}} \int_{f_{\min}}^{f_{\max}} T(f)df \tag{11}$$

The ratio of the transmission area filling F_T is described by equation (10).

2. Research

The theoretical study analyzed multilayers made of glass (layer A, $v_A = 4000\ [\mathrm{m/s}]$, $\rho_A = 3880\ [\mathrm{kg \cdot m^{-3}}]$) and epoxy resin (material B, $v_B = 2535\ [\mathrm{m/s}]$, $\rho_B = 1180\ [\mathrm{kg \cdot m^{-3}}]$) surrounded by water ($v_w = 1480\ [\mathrm{m/s}]$, $\rho_w = 1000\ [\mathrm{kg \cdot m^{-3}}]$) [7, 27]. The objective function was minimized for four frequency bands $[\mathrm{kHz}]$ in the ranges 0-5, 5-10, 10-15 and 15-20. The 40-layers structure were considered with a single layer thickness of 1 cm. Each population consisted of 20 structures.

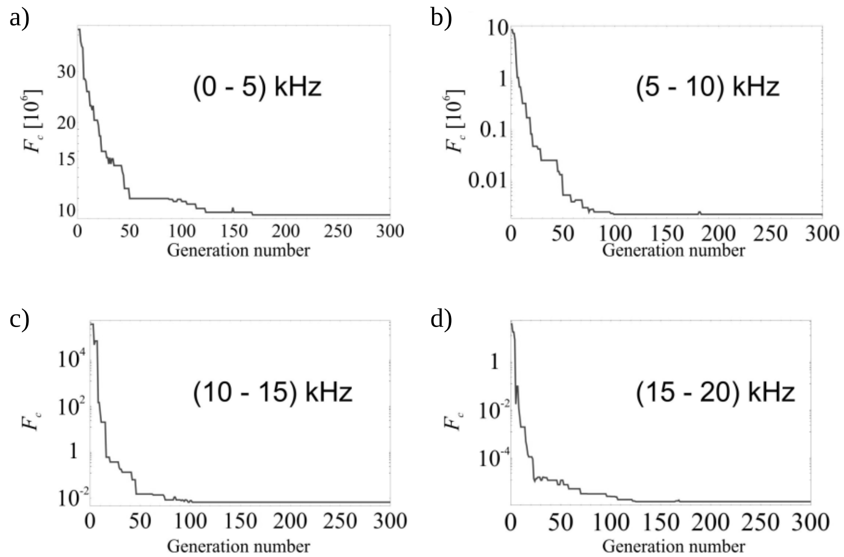

Figure 2. The objective function values of the best individuals (without normalisation) for each generation for subsequent analyzed bands

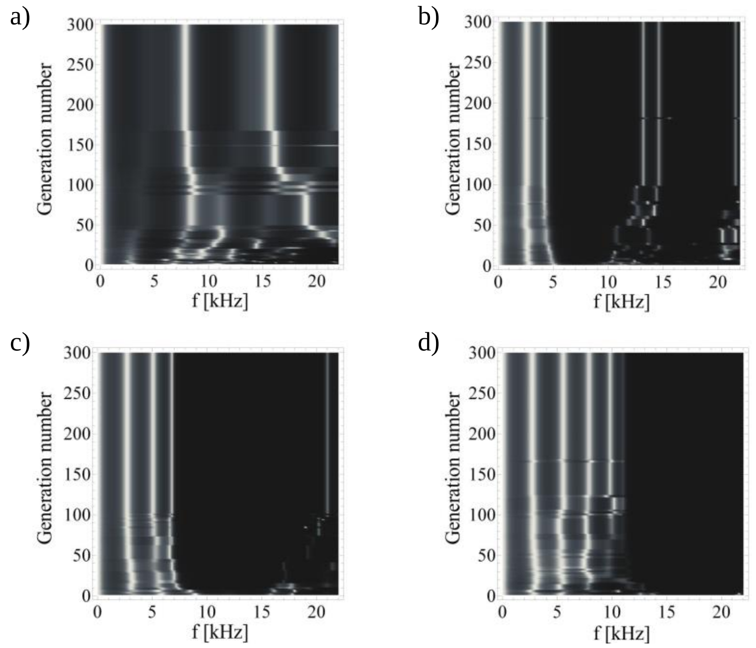

Figure 3. The density plots with transmission for the best individuals for each generation in searches for subsequent analyzed bands a) 0 kHz – 5 kHz, b) 5 kHz – 10 kHz, c) 10 kHz – 15 kHz, a) 15 kHz – 20 kHz

Fig. 2 shows how the function determined by equation (10) changed for the best structures of each generation. The value of the objective function on the graphs is presented on a logarithmic scale. Below 200 algorithm steps, the value of the objective function stabilized and the program reached the local minimum of solutions space. Small peaks after stabilization of the objective function were caused by the effect of the mutation on the entire population. Fig. 3 shows the transmission of structures with the lowest objective function from a given population. White means full transmission, and black means no transmission for a given frequency. The drawings show the evolutionary process and stabilization of the transmission structure after reaching the minimum of the objective function.

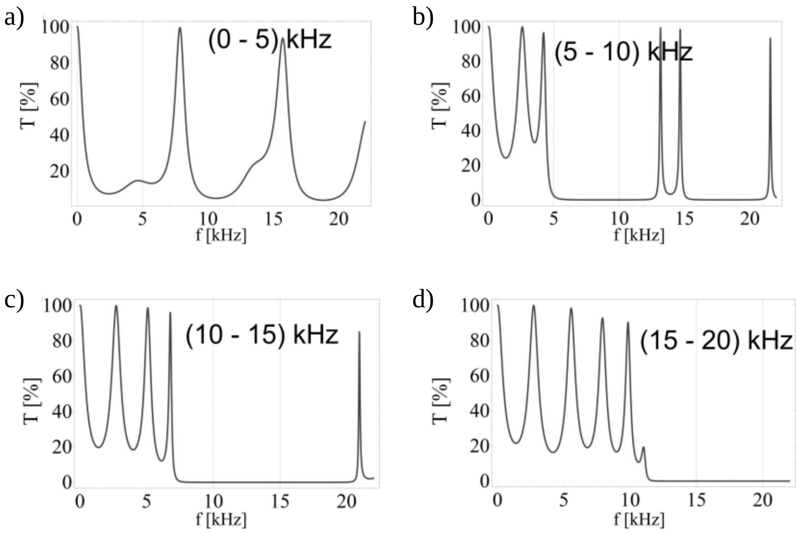

Figure 4. Transmission for the best found structures for each band a) 0 kHz – 5 kHz, b) 5 kHz – 10 kHz, c) 10 kHz – 15 kHz, a) 15 kHz – 20 kHz

Table 1. Best found structures for each band and the transmission integral for this band

Frequency range [kHz]	Transmission integral	Best found structure	Number of layers
0 – 5	$1.89 * 10^{-1}$	$A_{26}B_{14}$	2
5 – 10	$1.78 * 10^{-3}$	$A_7B_9A_9B_9A_6$	5
10 – 15	$5.81 * 10^{-6}$	$A_6B_5A_6B_5A_7B_5A_6$	7
15 – 20	$7.30 * 10^{-8}$	$A_3B_3A_4B_3A_4B_4A_4B_4A_4B_3A_4$	11

Fig. 4 presents transmission charts for structures with the minimum objective function value determined using a genetic algorithm. All graphs had high transmission peaks, but except for Fig. 4a, they had a low half width value. Table 1 shows the simplified notation of the structures found for the given bands (the value of subscript is the number of the layer repeats). It should be noted that the transmission integral in subsequent bands significantly decreases when the number of layers in the structure increases. The total structure thickness was constant for all cases.

3. Conclusions

The paper shows that it is possible to use a genetic algorithm to search for multilayer structures with given transmission properties. The algorithm allowed to find multilayer structures built of glass and epoxy resin for four frequency bands where the objective function was to reduce transmission and eliminate high transmission peaks with a small half width. Such structures can be used as mechanical wave filters and noise control devices.

In the work, finding the optimal assumed structure took less than 200 iterations of the algorithm. The higher the band the smaller the transmission integral in the analyzed frequency range. The high value of the transmission integral for a band below 5 kHz results from the fact that the structure is thin compared to the wavelength of the propagating mechanical waves in this frequency range. For higher frequency bands, the number of layers of the found structure increased.

It is planned to verify the obtained data by using 4 microphones impedance tube.

References

1. L. M. Brekhovskikh, *Waves in Layered Media, 2nd ed.,* Academic Press, New York, 1980.
2. P. Yeh, *Optical Waves in Layered Media*, John Wiley & Sons, New York, 1988.
3. J. Sapriel, B. Djafari-Rouhani, Vibrations in superlattices, Surf. Sci. Rep., **10** (1989) 189 – 275.
4. E. H. El Boudouti, B. Djafari-Rouhani, A. Akjouj, L. Dobrzynski, *Acoustic waves in solid and fluid layered materials*, Surf. Sci. Rep., **64** (2009) 471 – 594.
5. L. Dobrzynski et al., *Phononics*, Elsevier, 2017.
6. S. Garus, M. Szota, *Occurence of Characteristic Peaks in Phononic Multilayer Structures*, Revista de Chimie, **69**(3) (2018) 735 – 738.
7. S. Garus, W. Sochacki, M. Bold, *Comparison Of Phononic Structures With Piezoelectric $0.62Pb(Mg_{1/3}Nb_{1/3})O_3$-$0.38PbTiO_3$ Defect Layers*, Engineering Mechanics 2018 (red.) Fischer Cyril, Naprstek Jiri, Institute of Theoretical and Applied Mechanics of the Czech Academy of Sciences, Prague, (2018) 229 – 232.
8. A. M. Badreddine, J. H. Sun, F. S. Lin, J. C. Hsu, *Hybrid phononic crystal plates for lowering and widening acoustic band*, Ultrasonics, **54**(8) 2159 – 64.
9. S. Garus, M. Szota, *Band GAP Frequency Response in Regular Phononic Crystals*, Revista de Chimie, **69**(12) (2018) 3372 – 3375.
10. L. Han, Y. Zhang et al., *A modified transfer matrix method for the study of the bending vibration band structure in phononic crystal Euler beams*, Physica B: Condensed Matter, **407** (2012) 4579 – 4583.
11. S. Garus, M. Bold, W. Sochacki, *Transmission in the Phononic Octagonal Lattice Made of an Amorphous Zr55Cu30Ni5Al10 Alloy*, Acta Phys. Pol. A, **135**(2) (2019) 139 – 142.

12. S. Garus, W. Sochacki, M. Bold, *Transmission Properties of Two-Dimensional Chirped Phononic Crystal*, Acta Phys. Pol. A, **135**(2) (2019) 153 – 156.
13. M. N. Armenise, C. E. Campanella, C. Ciminelli, F. Dell'Olio, V. M. N. Passaro, *Phononic and photonic band gap structures: modelling and applications*, Physics Procedia, **3**(1) (2010) 357 – 364.
14. S. Garus, W. Sochacki, *One Dimensional Phononic FDTD Algorithm and Transfer Matrix Method Implementation for Severin Aperiodic Multilayer*, Journal of Applied Mathematics and Computational Mechanics, **16**(4) (2017) 17 – 27.
15. T. Miyashita, *Sonic crystals and sonic wave-guides*, Meas. Sci. Technol., (2005) 16, R47.
16. S. Alagoz, O. A. Kaya, B. B. Alagoz, *Frequency controlled wave focusing by a sonic crystal lens,* Applied Acoustics, **70** (2009) 1400 – 1405.
17. M. M. Sigalas, E. N. Economou, *Elastic and acoustic wave band structure,* Journal of Sound and Vibration, **158** (1992) 377 – 382.
18. C. Y. Qiu, Z. Y. Liu, Z. M. Jun, J. Shi, *Mode-selecting acoustic filter by using resonant tunneling of two-dimensional double phononic crystals*, Appl. Phys. Lett. **87** (2005) 104101.
19. A. Cicek, O. A. Kaya, M. Yilmaz, B. Ulug, *Slow sound propagation in a sonic crystal linear waveguide*, J. Appl. Phys., **111** (2012) 013522.
20. M. D. Zhang, W. Zhong, X. D. Zhang, *Defect-free localized modes and coupled-resonator acoustic waveguides constructed in two-dimensional phononic quasicrystals*, J. Appl. Phys., **111** (2012) 104314.
21. J. Sánchez-Dehesa, V. M. Garcia-Chocano, D. Torrent, F. Cervera, S. Cabrera, *Noise control by sonic crystal barriers made of recycled materials*, J. Acoust. Soc. Am., **129** (2011) 1173.
22. T. T. Wu, L. C. Wu, Z. G. Huang., *Frequency band-gap measurement of two-dimensional air/silicon phononic crystals using layered slanted finger interdigital transducers*, J. Appl. Phys., **97** (2005) 094916.
23. I. Kriegel, F. Scotognella, *Three material and four material one-dimensional phononic crystals*, Physica E 85 (2017) 34 – 37.
24. S. Villa-Arango, R. Torres, P. A. Kyriacou, R. Lucklum, *Fully-disposable multilayered phononic crystal liquid sensor with symmetry reduction and a resonant cavity*, Measurement, **102** (2017) 20 – 25.
25. G. A. Gazonas, D. S. Weile, R. Wildman, A. Mohan, *Genetic algorithm optimization of phononic band gap structures*, Int. J. Solids Struct., **43**(18) (2006) 5851 – 5866.
26. H. W. Dong, X. X. Su, Y. S. Wang, C. Zhang, *Topological optimization of two-dimensional phononic crystals based on the finite element method and genetic algorithm*, Struct. Multidiscip. Optim., **50**(4) (2014) 593 – 604.
27. S. Garus, W. Sochacki, *High-performance quasi one-dimensional mirrors of mechanical waves built of periodic and aperiodic structures*, J. App. Math. Comp. Mech., **17**(4) (2018) 19 – 24.